Desalination and Water Treatment
www.deswater.com

doi: 10.5004/dwt.2017.21295

86 (2017) 191–202
August

Efficient removal of methylene blue dye using mangosteen peel waste: kinetics, isotherms and artificial neural network (ANN) modeling

Asma Nasrullah[a], A.H. Bhat[a,*], Mohamed Hasnain Isa[b], Mohammed Danish[c], Abdul Naeem[d], Nawshad Muhammad[e], Taimur Khan[b]

[a]*Fundamental and Applied Sciences Department, Universiti Teknologi PETRONAS (UTP), 32610 Bandar Seri Iskandar, Perak, Malaysia, emails: aamir.bhat@utp.edu.my (A.H. Bhat), advent_chemist@yahoo.com (A. Nasrullah)*
[b]*Department of Civil and Environmental Engineering, Universiti Teknologi PETRONAS (UTP), 32610 Bandar Seri Iskandar, Perak, Malaysia, emails: hasnain_isa@utp.edu.my (M.H. Isa), taimurkhan7@gmail.com (T. Khan)*
[c]*Technical Foundation Section, Malaysian Institute of Chemical and Bio-Engineering and Technology (MICET), Universiti Kuala Lumpur (UniKL), Perindustrian Bandar, Taboh Naning, Alor Gajah 78000, Melaka, Malaysia, email: mdanishchem@googlemail.com*
[d]*National Centre of Excellence in Physical Chemistry, University of Peshawar, Peshawar, Pakistan, email: naeeem64@yahoo.com*
[e]*Interdisciplinary Research Centre in Biomedical Materials, COMSATS Institute of Information Technology, Lahore, Pakistan, email: nawshadchemist@yahoo.com*

Received 24 December 2016; Accepted 4 August 2017

ABSTRACT

In this work, mangosteen peel (MP) waste was used as a new biosorbent for removal of methylene blue (MB) dye from aqueous solution. Surface area, surface functional groups, surface charge and surface morphology were analyzed through Brunauer Emmett Teller, Fourier transform infrared, pH_{zpc} and field emission scanning electron microscopy/energy dispersive X-ray spectroscopy techniques, respectively. The major functional groups were –CO, –COO and –OH. Batch adsorption experiments were conducted with varying MP dose (0.01–0.08 g), pH (2–12), contact time (10–60 min), temperature (25°C–45°C) and concentration of MB solution (50–150 mg/L). The study examined the implementation of artificial neural network for the prediction of MB adsorption from aqueous solution by MP, based on 30 experimental sets of batch adsorption study. Optimum number of neurons determined was 4 for Levenberg–Marquardt training algorithm; at which the highest value of R^2 and lowest mean square error were found to be 0.997 and 2.972, respectively. Among the various kinetic models applied, the pseudo-second-order kinetic model was identified to be the most suitable to represent the adsorption of MB on the surface of MP. Langmuir, Freundlich, Temkin and Harkins–Jura isotherm models were employed to study the adsorption equilibrium. Langmuir isotherm model was identified as the most suitable. The calculated values of thermodynamic factors, $\Delta S°$, $\Delta G°$, $S*$, E_a and $\Delta H°$, showed that the adsorption phenomenon is spontaneous, feasible and endothermic in nature.

Keywords: Mangosteen peel; Methylene blue; Artificial neural network; Adsorption capacity; Kinetic models; Thermodynamic parameters

1. Introduction

Rapid increase in population, industries and unplanned urbanization contribute to water pollution [1,2]. It is estimated that about 7–10 × 10^5 tons of dyes are produced annually worldwide and widely utilized in different industries such as paper, textile finishing, food coloring, carpet, leather, plastics, cosmetics and printing [3,4]. The presence of dyes in water has an adverse effect on aquatic and terrestrial biota including human beings due to their toxic and carcinogenic nature [5]. Even, the presence of a small concentration of dyes in

* Corresponding author.

water sources is highly noticeable and unwanted. Methylene blue (MB), a cationic dye, is most commonly utilized to colorize plastic, cotton and wood. The dye has been declared as a hazardous material as it can cause many diseases like vomiting, diarrhea and skin irritation [6]. Therefore, the effective MB removal from water is an important environmental issue to be considered.

Biological, physical and chemical treatment technologies available for removing dyes from wastewater include bacterial degradation, flocculation, photocatalytic mineralization, etc. However, these methods have some drawbacks, which involve cost, time and need of expertise for operation. Wastewater containing synthetic dyes in low concentration cannot be efficiently removed by these methods. Among the many methods applicable for dye removal, adsorption is a well-known heterogeneous separation technique, which is easily applied, economical, non-toxic, simple and efficient for removing various types of dyes even in low concentration from wastewater [6–9]. In recent years, different types of adsorbents such as zeolites [10], geopolymers [11], kapok [12], cellulose [13], cotton [14] and clay have been used to eliminate dyes from dye-polluted water. The utilization of biowastes as adsorbents has attracted great attention owing to their low price, non-toxic nature, easy availability, etc. [15].

In this research work, due to abundance in Malaysia, mangosteen peel (MP) was used as an adsorbent for the elimination of MB from aqueous solution. The botanical name of mangosteen is *Garcinia mangostana*. It belongs to the Clusiaceae family and *Garcinia* genus. According to the Malaysian Ministry of Agricultural and Agro-Based Industry mangosteen production estimated was 29,520 ton/year in 2010, which in turn produced 17,712 ton of MPs. In fact, each kilogram of mangosteen can produce 0.6 kg MP, which is simply discarded/thrown unsafely in open space, and left to rot and produce putrescible smell due to the hot and humid environment in Malaysia. The objective of the current research work is to investigate the use of this abundantly available agricultural waste as an adsorbent for MB removal from aqueous solution. Hence, addressing the waste disposal as well as dye pollution problems simultaneously.

Presently, artificial neural network (ANN) modeling has been shown to be an efficient method to develop a complex relationship between variables. ANN has been used by various researchers for the prediction of dyes and heavy metals adsorption. However, limited research has been reported, which analyses the use of ANN for MB dye adsorption onto biomass from aqueous solution [19,20]. ANN is an important technique to validate the experimental adsorption based on predicted adsorption, generated by ANN model. This study examined the implementation of ANN for the prediction of MB adsorption from aqueous solution by MP. The batch adsorption data (dose, pH, concentration and temperature) was analyzed using ANN; the experimental and predicted values were found to agree very well with each other. Surface morphology and functional groups determination were conducted using field emission scanning electron microscopy (FESEM) and Fourier transform infrared (FTIR) spectroscopy, respectively. The effects of MPs dose, pH of the solution, contact time, dye concentration and temperature were studied in dye removal process. Adsorption kinetics, isotherms and thermodynamic studies were conducted and reported.

2. Experimental

2.1. Preparation of adsorbent and dye solution

MPs were obtained from a local market and dried at 45°C for 48 h in an oven. The dried peels were ball milled into powdered form, washed with distilled water twice and dried at 45°C in an oven for 24 h and kept in a glass bottle for further use. A stock solution of MB was prepared by dissolving 1.000 ± 0.005 g of MB into 1 L of distilled water. The working solutions of MB were prepared by diluting the stock solution to desired concentration levels.

2.2. Characterization of adsorbent

The functional groups on the surface of MP before and after sorption of MB dye were determined using FTIR spectroscopy (PerkinElmer, Frontier, USA). The FTIR spectra were measured in the range of 4,000–400 cm^{-1} with five resolution using KBr disk technique. Surface morphology of MP was studied by FESEM using a JEOL-6700F, operated at the acceleration voltage of 10 kV and filament current of 60 mA. Surface area of MP was determined by nitrogen adsorption–desorption isotherms using a surface area analyzer (Micromeritics ASAP 2020). The total pore volume was estimated to be the volume of liquid nitrogen adsorbed at a relative pressure of 0.98. Salt addition method was used to determine point of zero charge (PZC) of MP. In this method, 0.01 M solution $NaNO_3$ was prepared in distilled water. 0.2 g of MP was added to 40 mL of 0.01 M $NaNO_3$ solutions in different titration flasks and pH was adjusted to 2, 3, 4, 5, 6, 7, 8, 9, 10, 11 and 12 using 0.01 M NaOH and 0.01 M HNO_3 solutions. The flasks were then shaken for 24 h to reach equilibrium. The resulting pH values were measured. The plot of ΔpH (the difference between initial and final pH) vs. initial pH gave the PZC value (the point where pH = 0).

2.3. Batch adsorption tests

To investigate the sorption of MB by MP, batch adsorption tests were performed using aqueous solutions of MB. Effect of MPs dose (0.02–0.08 g), initial MB dye concentration (50–150 mg/L), pH (2–12), temperature (298.15 K to 318.15 K) and contact time (10–150 min) were evaluated. Table 1 shows the overall summary of experimental design. The MB adsorption experiment was performed in 100 mL Erlenmeyer flasks with 25 mL dye solution. The flasks were agitated using an orbital shaker at 150 rpm. The summary of experimental design is given in Table 1.

After shaking for desired time, the solid phases were separated by filtration and the concentration of MB in supernatant solution was measured by UV–Vis spectroscopy (double beam UV–Visible spectrophotometer, Shimadzu 1800) at 664 nm with the regression coefficient of the standard plot (0.995). The percentage removal (% R) and adsorption capacity (q_t) of MB were calculated using Eqs. (1) and (2), respectively [16]:

$$\%R = \left[\frac{C_0 - C_t}{C_0}\right] \times 100 \quad (1)$$

$$q_t = \left[\frac{(C_0 - C_t)}{M} \times V\right] \quad (2)$$

Table 1
Summary of experimental design

C_i (ppm)	Amount of MPs (g)	pH	Time (min)	T (°C)
50	(0.01, 0.02, 0.04,0.06, 0.08)	7	60	25
50	0.01	(2, 4, 6, 8, 10, 12)	60	25
50, 100, 150	0.01	10	(10, 20, 30, 60, 90, 120)	25
50	0.01	10	60	(25, 35, 45)

where C_0 is the initial the concentration of MB, C_t is the concentration of MB at any time, q_t is the adsorption capacity at any specific time, V is the volume of MB solution in liter and M is the mass of MPs utilized.

2.4. Adsorption kinetic, isotherm and thermodynamic studies

Kinetic models, adsorption isotherms and thermodynamic parameters were evaluated to determine the rate of adsorption, the maximum adsorption capacity of the MP and enthalpy and spontaneity of adsorption of MB on MP. For kinetics study, the pseudo-first-order [17], pseudo-second-order, intraparticle diffusion [18] and Elovich [19] models were applied. To analyze the interaction of MB dye with MP, Langmuir [20], Freundlich [21], Temkin [22] and Harkins–Juar [23] isotherms were studied. Thermodynamic parameters, namely, change in standard enthalpy ($\Delta H°$), standard Gibbs free energy ($\Delta G°$) and standard entropy ($\Delta S°$) were calculated from experimental adsorption data recorded from 25°C to 45°C.

2.5. Artificial neural network

ANN is a data processing tool that consists of many units called neurons or nodes. Neurons are arranged in layer and within the layers; these neurons are connected to each other by weights and biases. The first layer is termed as input layer and the last layer is the output layer. There is another layer between these two layers that is known as hidden layer. In ANN architecture, the number of input neurons is equal to the number of input variables. Whereas, the output neurons are the desired output variables from the network. Three stages are needed to be considered during ANN applications, namely (1) training, (2) validation and (3) testing. In training and validation stages, both the input and the target data are introduced to the model, while only input data are considered by the model in the testing stage [14]. The network architecture used in this study is shown in Fig. 1.

2.6. Selection of optimum number of neurons

In this study, a three-layered backpropagation neural network with tangent sigmoid transfer function (tansig) at hidden layer and a linear transfer function (purelin) at output layer was used. Neural network toolbox of MATLAB R2013a software was used to develop the ANN model to describe MB adsorption. To determine the optimum number of neurons that can accurately predict the adsorption of MB on to MP based on 40 experimental sets of batch study, different number of neurons were tested. The optimization for

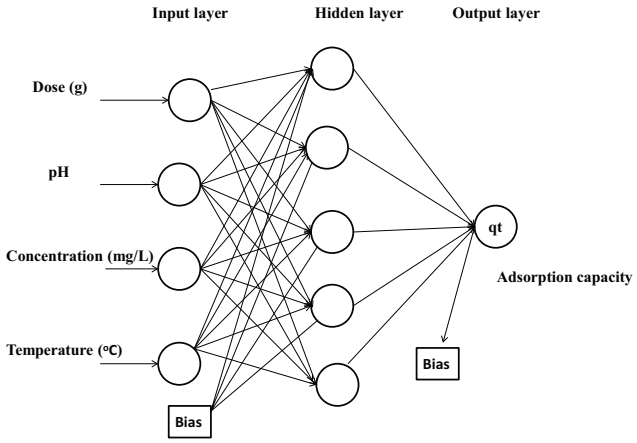

Fig. 1. Artificial neural network archtecture.

Levenberg–Marquardt (LM) training algorithm was done by varying the number of neurons in the range of 4–40. It was found that at 16 number of neurons yielded the lowest mean square error (MSE) of 0.0017 and highest R^2 of 0.99.

3. Results and discussion

3.1. Physical characteristics of MPs

FESEM is a useful technique to study the morphological properties and surface features of materials. The SEM images of MP (Fig. 2(A)) show the difference in morphology of MP before and after MB adsorption. Before adsorption of MB dye, MP exhibited rough and uneven surface with irregular wide spaces (cavities). This uneven surface is assumed to be the area of interaction which facilitates the adsorption of dye molecules from aqueous solution. On the other hand, the surface became homogenous and smooth after adsorption of MB molecules, due to the coverage of surface and pores of MP with MB molecules. The same phenomenon was also observed for the adsorption of MB using different adsorbents [24]. Energy dispersive X-ray spectroscopy (EDX) spectra showed increase in nitrogen content of MP after MB adsorption; confirming the adsorption of MB on MP (Fig. 2(B)).

FTIR is an important technique which gives information about the characteristic functional groups present on the surface of adsorbent, which make the adsorption process possible. The FTIR spectra of MP before and after MB adsorption are shown in Fig. 3(A). The spectra contain many adsorption peaks, which indicate the complexity of MP. The presence of a broad peak at 3,433 cm^{-1} is due to the stretching vibration of –OH groups present on the surface of MP. The presence

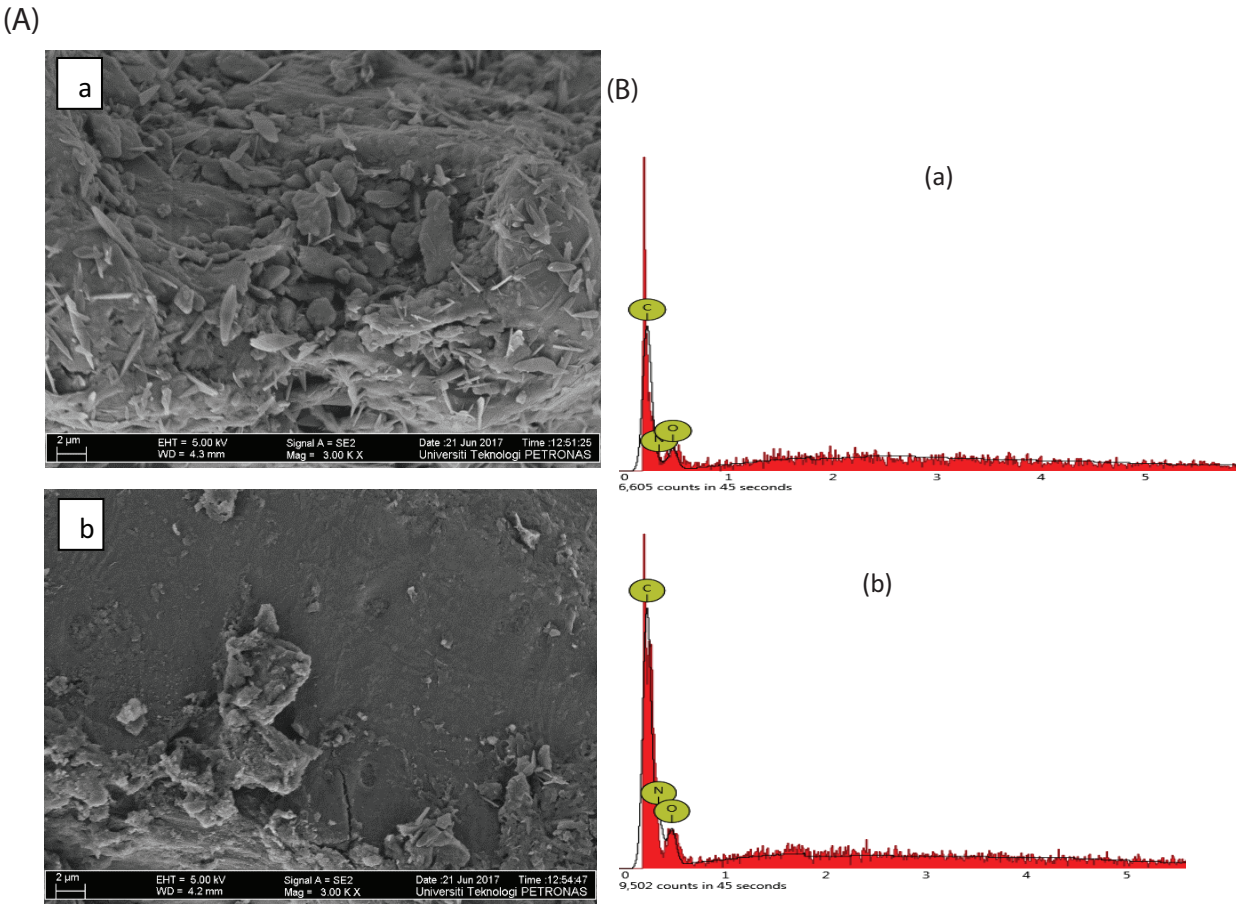

Fig. 2. (A) SEM image of MP (a) before and (b) after MB adsorption. (B) EDX spectra of MP (a) before and (b) after MB adsorption.

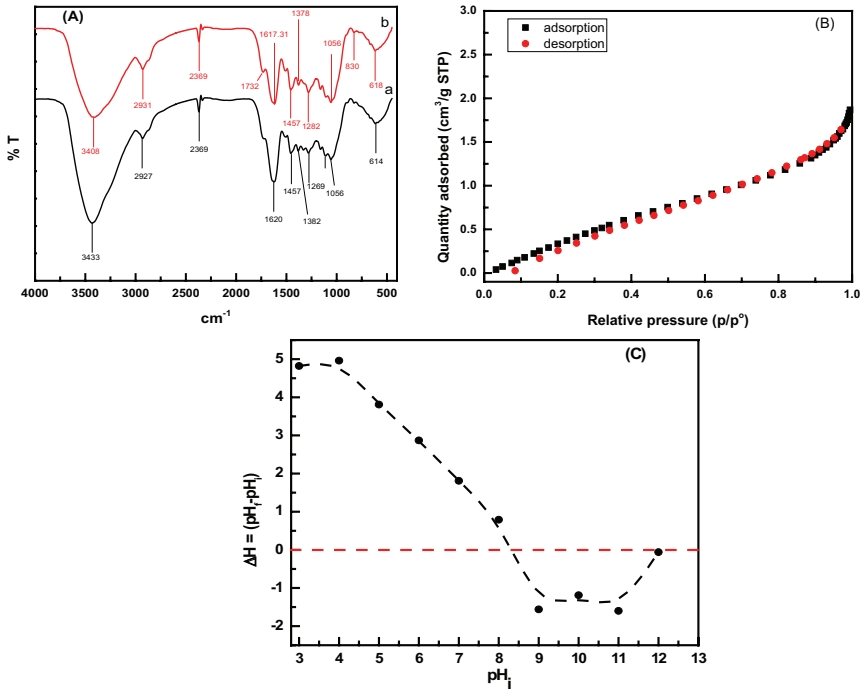

Fig. 3. (A) FTIR spectra of MP (a) before and (b) after MB adsorption, (B) N_2 adsorption–desorption of MP and (C) P_{ZC} of MP.

of a broad band at 2,927 cm^{-1} is assigned to the asymmetric stretching vibration of methyl $–CH_3$ groups. The stretching vibration of carbonyl (–C=O) group with intermolecular –H bond appeared at 1,620 cm^{-1}. The peak at 1,457 cm^{-1} indicates the presence of $–CH_3$ symmetric bending. The presence of a peak at 1,382 cm^{-1} is due to the existence of $–CH_2$ and $–CH_3$ groups. The FTIR analysis shows MP containing a large number of hydroxyl and carboxylic groups, which are considered as active sites for interaction and therefore make the adsorption of cationic dyes possible. Fig. 3(A) shows that after MB adsorption, the stretching vibration peak of –OH and carbonyl (–C=O) groups with intermolecular hydrogen bonding are shifted from 3,433 to 3,408 cm^{-1} and from 1,620 to 1,617.31 cm^{-1}, respectively. This observation is in line with previous study.

N_2 adsorption–desorption isotherm for MP is shown in Fig. 3(B). The texture properties for MP using N_2 adsorption–desorption isotherm is given in Table 2. According to the IUPAC system, the isotherm is type II. This sample has very low pore volume and therefore yielded type II isotherm.

3.2. Effect of operating factors

3.2.1. Effect of solution pH

pH of solution plays an effective role in the uptake of MB molecules from aqueous solution. The pH of dye solution provides the information about the cationic (pH = 0–6.9) or anionic (pH = 7.1–14) charged species. The presence of charge centers on both adsorbate and adsorbent are very important in deciding the favorability of adsorption by either deprotonation or protonation resulting in the attraction or repulsion of their counter ions. The effect of pH on the adsorption of MB was studied in the pH range of 2–12 at 25°C with an initial MB concentration 50 mg/L and adsorbent dose 0.02 g. The adsorption capacity of MP as functions of pH of the solution is shown in Fig. 4(a). The results demonstrated that with the increase of pH of the solution from 2 to 10, the adsorption (%) and adsorption capacity of MB increased from 61.93% to 98% and from 38.7 to 61.2 mg/g, respectively. At acidic pH (below pH 6), the existence of the excess amount of H^+ competes with MB molecules for the binding sites present on the MP surface, which leads to decrease in uptake of MB from aqueous solution. At higher pH (above pH 7), the functional groups of the adsorbent become more negatively charged resulting in the increase of electrostatic interaction between counter ions of MPs and MB dye. Therefore, it was concluded that pH value of 10 is optimal for the dye removal from aqueous solution. Hameed and Ahmad [25] also found the maximum adsorption capacity of MB dye on garlic peel at pH 10.

The results are also in good agreement of point of zero charge (P_{ZC}) of MP, which is found to be 8.3 as shown in Fig. 3(C). At this pH_{pzc}, the surface charge of MP is zero. Therefore, at pH < pH_{pzc}, the MP carries net positive charge decreasing the uptake of cationic MB dye from aqueous solution. While at pH > pH_{pzc}, the presence of H^+ ions are decreased in the solution due to increasing pH of the solution. At basic pH the functional groups are more negatively charge which in turn increase the adsorption of MB from aqueous solution. Fig. 4(a) shows that the experimental values are in good agreement with the ANN predicted values.

Table 2
Texture properties of mangosteen peel waste

S_{BET} (m^2/g)	3.787
Pore volume (cm^3/g)	0.00289
Pore width (Å)	30.517
Pore diameter (Å)	57.87

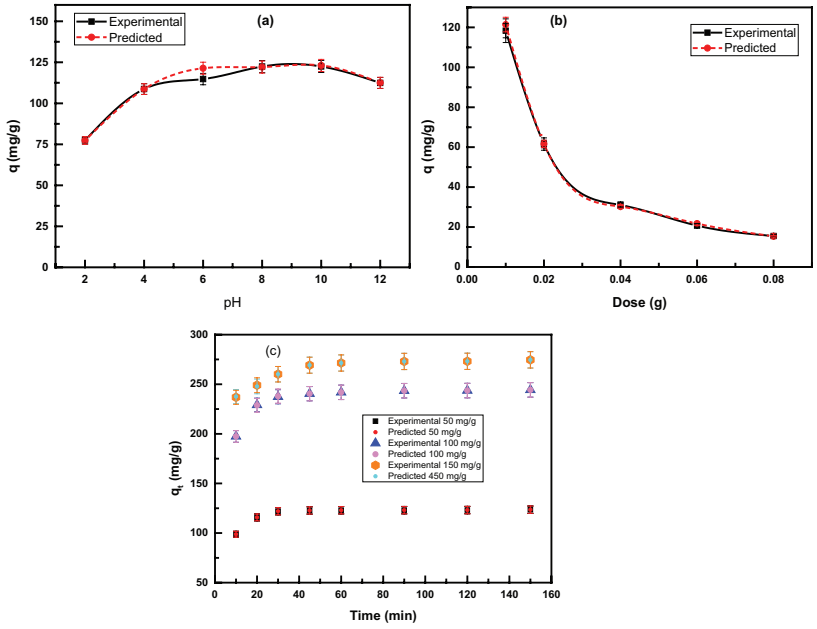

Fig. 4. Effect of (a) pH of solution, (b) adsorbent dose and (c) time and dye concentration on the adsorption capacity of MP.

3.2.2. Effect of adsorbent dose

The effect of adsorbent dose on dye removal was studied with amounts of MP ranging from (0.01 to 0.08 ± 0.005 g) with an initial MB concentration 50 mg/L, contact time 60 min and using optimal pH of 10. The result demonstrated that with an increase in MP dose from 0.01 to 0.08 g, the percentage removal of dye increased from 94.67% to 99.42%. However, there is no considerable change in percentage removal of MB when adsorption dosage increased from 0.06 to 0.08 g; indicating that adsorption was almost completed.

Fig. 4(b) shows that with an increase in MP dose from 0.01 to 0.08 g, adsorption capacity decreased from 118.34 to 15.50 mg/g. Maximum adsorption capacity of MB was observed using 0.01 g of MP dose. The increase in percentage removal of MB with MP dose is due to the availability of more binding sites on the surface of MPs for dye molecules. However, with the increase of adsorbent dose the adsorption capacity decreased due to the inverse relation between the adsorbent dose and adsorption capacity as shown in Eq. (2). At higher adsorbent dose, the decrease in adsorption capacity is attributed to the excess adsorption sites available.

3.2.3. Effect of contact time and initial MB concentration

The effect of contact time (10–150 min) and initial concentration of MB (50–150 mg/L) on adsorption capacity was investigated at the optimal pH of 10 and adsorbent dose of adsorbent (0.01 g). The obtained results are graphically presented in Fig. 4(c). The result illustrates that the process of adsorption is rapid and equilibrium was achieved within 60 min as indicated no increase in q_e with further increase in contact time. The initial rapid increase in q_t is due to the availability of free binding sites on MP for MB ions to interact with and bind, while at a longer contact time, the maximum adsorption capacity was constant due to saturation of active sites of the adsorbent. Similar trend has also been reported in the literature [26].

To examine the effect of initial dye concentration on adsorption capacity under optimal conditions, three different solution concentrations (50, 100 and 150 mg/L) were used and the obtained results are shown in Fig. 4(c). The data indicate that the adsorption capacity increased from 123.01 to 272.99 mg/L with an increase in MB concentration from 50 to 150 mg/L. This increase in adsorption capacity with the increase of the initial concentration of dye is due to the availability of more dye molecules to adsorb on MP. Another possible reason for the increase in adsorption capacity with an increase in adsorbate concentration was the higher mass transfer driving force that caused increased interaction between MB molecules and the adsorbent. Fig. 4(c) shows the ANN predicted values and experimental values of MB adsorption on MP are very close to each other. Thus, ANN model can predict the adsorption of MB dye on MP precisely.

3.3. Kinetic study of adsorption

The kinetics study of adsorption is important to calculate the mechanisms involved in the process. Four kinetic models, namely, Langenargen pseudo-first-order, pseudo-second-order, intraparticle diffusion and Elovich models were evaluated. Eq. (3) represents the linear form of pseudo-first-order kinetic model:

$$\log\left(q_e - q_t\right) = \log q_e - \frac{k_1}{2.303}t \tag{3}$$

where k_1 (min^{-1}) is the rate constant for pseudo-first-order model, t (min) is contact time and q_e (mg/g) and q_t (mg/g) are the amounts of MB adsorbed at equilibrium and at any time, respectively. The pseudo-first-order kinetic model shows a direct relationship between $\log(q_e - q_t)$ and t (Fig. 5(a)), allowing determination of the values of k_1 and q_e from the slope and intercept, respectively.

The linear form of pseudo-second-order kinetic model can be written as:

$$\frac{t}{q_t} = \frac{1}{k_2 q_e^2} + \frac{t}{q_e} \tag{4}$$

where k_2 (g/mg min) is the rate constant for pseudo-second-order kinetics. The plot of t/q_t against time t gives a straight line with slope $1/q_e$ and intercept $1/k_2q_e^2$ (Fig. 5(b)). The values of kinetic coefficients obtained for pseudo-first-order and pseudo-second-order kinetic models along with regression coefficient (R^2) are listed in Table 3. The values of regression coefficient for adsorption of MB using pseudo-first-order and pseudo-second-order kinetic models are 0.887 and 0.999, respectively. The result demonstrates that the adsorption of MB on MP using pseudo-second-order model not only shows very good curve fitting in term of regression coefficient (R^2 = 0.999) R^2, but also shows good agreement between experimental and calculated values of adsorption capacity.

The intraparticle diffusion model is an important kinetic model mostly used for explanation of diffusion mechanism of adsorption. The intraparticle diffusion model is as shown in Eq. (5):

$$q_t = k_{\mathrm{id}} t^{0.5} + C \tag{5}$$

where k_{id} (mg/g min) is the rate constant for intraparticle diffusion and C is intercept of the line with the q_t axis and indicates boundary layer thickness [27]. The plot for q_t vs. $t^{0.5}$ is shown in Fig. 5(c) and the obtained data are summarized in Table 4. The low values of regression coefficient (R^2: 0.5244–0.2589) suggest that intraparticle diffusion model does not represent the adsorption of MB on MP. The positive values of intercept reflect larger boundary effect and processes involved in adsorption other than intraparticle diffusion. Initially, the boundary of the interface was thin so the rate of diffusion should be faster; as interface boundary becomes thicker, the diffusion rate should decrease.

Another important kinetic model based on adsorption capacity is the Elovich model which assumes that the adsorption sites increase exponentially with adsorption, implying multilayer adsorption. Elovich model is mathematically shown in Eq. (6):

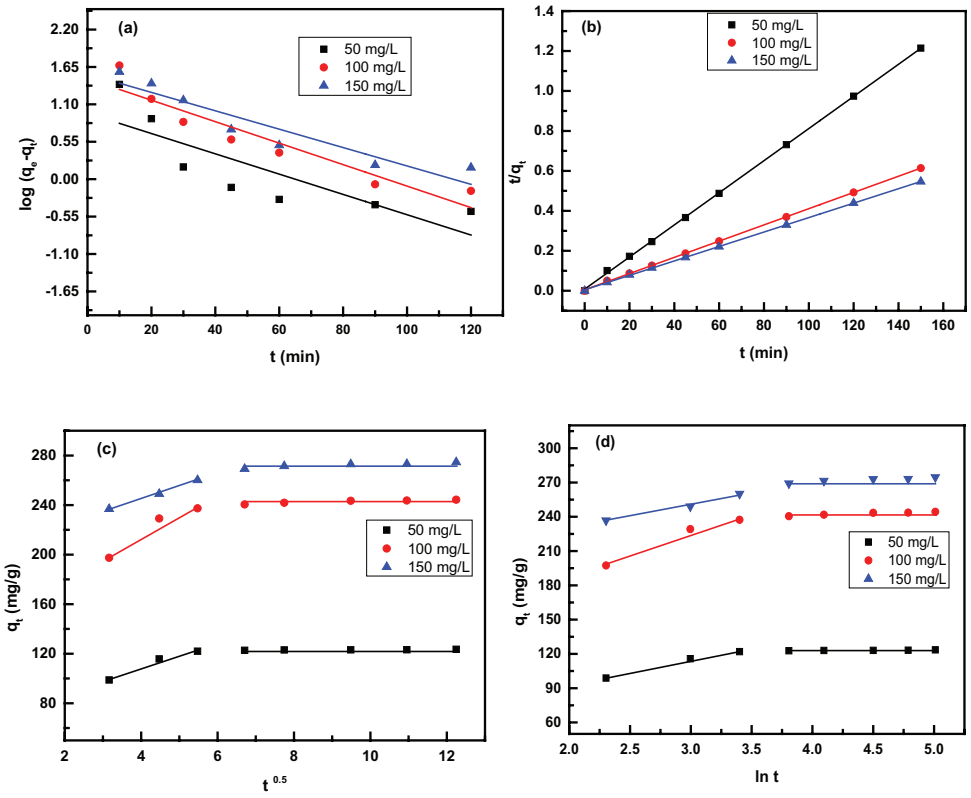

Fig. 5. (a) Pseudo-first–order, (b) pseudo-second–order, (c) intraparticle diffusion and (d) Elovich plots for MB adsorption on MP.

Table 3
Kinetics parameters for adsorption of MB on MPs using pseudo-first-order and pseudo-second-order models

C_0	Pseudo-first-order kinetic				Pseudo-second-order kinetic		
	q_{exp} (mg/g)	q_{cal} (mg/g)	k_1 (min^{-1})	R^2	q_{cal} (mg/g)	k_2 (g min/mg)	R^2
50	123.01	9.3269	0.03436	0.632	124.37	0.007816	0.999
100	241.86	29.9847	0.03636	0.871	246.30	0.003391	0.999
150	271.44	35.1625	0.03111	0.864	277.00	0.002692	0.999

Table 4
Kinetics parameters for MB adsorption on MPs using intraparticle and Elovich models

C_0	Intraparticle diffusion model			Elovich model			
	C	k_{pi}	R^2	β	A	k_1 (g min/mg)	R^2
50	109.887	0.235	0.5244	8.259	265,504.53	0.00475	0.8824
100	216.370	0.474	0.3488	16.124	604,425.19	0.00210	0.7405
150	248.237	0.427	0.2589	13.653	64,345,068	0.00209	0.6539

$$q_t = \frac{1}{\beta}\ln(\alpha.\beta) + \frac{1}{\beta}\ln(t) \quad (6)$$

where α (g/g min) is the initial adsorption rate and β (g/g) is the adsorption constant. A plot of q_t against ln(t) gives a straight line with a slope 1/β and intercept (1/β) ln(αβ). The Elovich plot is shown in Fig. 5(d) and the values of constants are listed in Table 3. The lower values of regression coefficient indicate that the covering of adsorption sites that implies multilayer adsorption does not follow the adsorption of MB onto MP in the studied concentration range. The similar trend has been studied by other researchers elsewhere [28].

3.4. Thermodynamic study

3.4.1. Effect of temperature

The effect of temperature on dye removal onto MP was studied at 25°C, 35°C and 45°C under optimized

experimental conditions (adsorbent dose 0.01 g, pH 10 and t 60 min). The temperature effect on the capacity of adsorption is presented in Fig. 6(a). The adsorption capacity was found to be 118.34, 119.03, 119.90, 120.54 and 121.20 mg/g at 25°C, 30°C, 35°C, 40°C and 45°C, respectively. High temperature may produce a swelling effect within the internal structure of MP enabling MB molecules to penetrate further [29]. The increase in the capacity of adsorption of dye onto MP at higher temperature indicates the endothermic nature of the adsorption.

To examine the spontaneity, randomness and heat of adsorption of MB on MP, various thermodynamic parameters, namely, change in standard Gibbs free energy ($\Delta G°$), standard entropy ($\Delta S°$) and standard enthalpy ($\Delta H°$) were estimated by the following equations:

$$K_c = \frac{q_e}{C_e} \tag{7}$$

$$\Delta G^0 = -RT \ln K_c \tag{8}$$

$$\ln K_c = \frac{\Delta S^0}{R} - \frac{\Delta H^0}{RT} \tag{9}$$

where K_c is the equilibrium constant, T is the absolute temperature (K) and R (8.314 J/mol K) is the universal gas constant. The values of $\Delta H°$ and $\Delta S°$ can be calculated from the slope and intercept of the linear plot of $\ln K_c$ vs. $1/T$ (Fig. 6(b)). The change in Gibbs free energy can be determined using Eq. (8). The obtained values of thermodynamic parameters are summarized in Table 5. The negative value of $\Delta G°$ for adsorption of MB on MP at all temperatures indicates the feasibility and spontaneity of the process. The chemical or physical nature of adsorption could be recognized by the $\Delta G°$ value of the process. If $\Delta G°$ value lies in range of 0–20 kJ/mol, the adsorption is physical in nature, while if $\Delta G°$ is within the range from –80 to –400 kJ/mol, the process can be assigned as chemical adsorption [30].

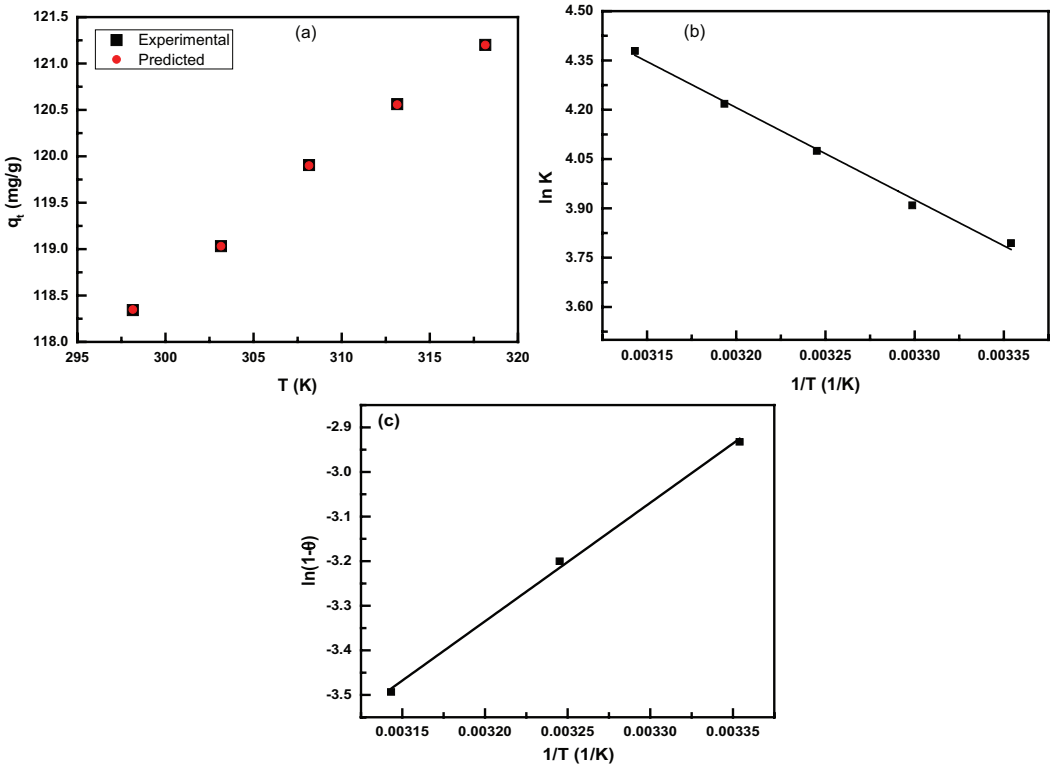

Fig. 6. (a) Arrhenius plot, (b) van't Hoff and (c) sticking probability plot for MB adsorption on MP.

Table 5
Thermodynamics parameters for MB adsorption on MP

T (K)	$\Delta G°$ (kJ/mol)	$\Delta H°$ (kJ/mol)	$\Delta S°$ (J/mol K)	R^2	S^*	E_a (kJ/mol)
298.15	–9.40	23.447	109.51	0.993	7.21×10^{-6}	22.10
303.15	–9.85					
308.15	–10.44					
313.15	–10.98					
318.15	–11.58					

Kumar and Barakat [31] described the criteria for physical adsorption based on $\Delta H°$: 4–10 kJ/mol (van der Waals forces), 5 kJ/mol (hydrophobic bonding forces), 2–40 kJ/mol (hydrogen bonding forces), 40 kJ/mol (coordination exchange), 2–29 kJ/mol (dipole bonding forces) and 60 kJ/mol (chemical adsorption). The positive change in $\Delta H°$ (23.040 kJ/mol) and $\Delta S°$ implies that MB adsorption on MP is endothermic and spontaneous in nature [32]. It is thus, assumed from the $\Delta H°$ value that the adsorption of MB on MP is due to physical interaction.

To further confirm that physical adsorption is predominant, the sticking probability (S^*) and activation energy (E_a) values were calculated by applying modified Arrhenius Eq. (10) related to surface coverage (θ) as follows [33]:

$$S^* = (1-\theta)e^{-E_a/RT} \tag{10}$$

$$\theta = \left[1 - \frac{C_e}{C_0}\right] \tag{11}$$

$$\ln(1-\theta) = \ln S^* + \frac{E_a}{RT} \tag{12}$$

where θ is the surface coverage and is equal to $1 - C_e/C_0$. The values of S^* and E_a can be estimated from the intercept and slope by plotting $(1 - \theta)$ vs. $1/T$ (Fig. 6(c)). The value of S^* must lie in the range $0 < S^* < 1$ for the process to be probable and depend on the temperature of the system. The values of S^* and E_a are 7.21×10^{-6} and 22.10 kJ/mol, respectively. The parameter S^* represents the potential of MB to remain on the surface of MP to be indefinite [34]. The positive value of E_a is an indication of endothermic nature of adsorption and therefore occurs at a high temperature of the solution.

3.5. Isotherm study

This study was conducted to correlate the capacity of adsorption and the residual concentration of MB molecules present in the solution. Four isotherm models were used, namely, Langmuir [20], Freundlich [21], Temkin [22] and Harkins–Juar [23] isotherms. Langmuir isotherm model assumes that the adsorbent surface contains homogeneous binding sites having identical adsorption energies and involves monolayer adsorption of MB. The linear form of Langmuir isotherm can be written as:

$$\frac{C_e}{q_e} = \frac{1}{bQ_0} + \frac{1}{Q_0}.C_e \tag{13}$$

where Q_0 (mg/g) is the capacity of adsorption and b (L/mg), called Langmuir constant, represents the energy of the sorption process.

Freundlich isotherm is an empirical relationship between q_e and C_e that assumes heterogeneity of the system. The Freundlich constants K_F and n can be calculated from the following linear form of the isotherm:

$$\ln q_e = \ln K_F + \frac{1}{n}\ln C_e \tag{14}$$

where K_F is Freundlich constant and n is the intensity of adsorption. $1/n$ value indicates sorption favorability, $n > 1$ shows favorable adsorption condition.

Temkin isotherm model can be linearized as:

$$q_e = B\ln A + B\ln C_e \tag{15}$$

where A and B are Temkin isotherm constants (L/g) and the heat of adsorption (J/mol), respectively. Their values can be obtained from the intercept and plot of q_e vs. $\ln C_e$ [11].

The straight form of Harkins–Jura isotherm model assumes multilayer adsorption and could be explained by the presence of heterogeneous pore distribution. Its linear form is given in Eq. (16):

$$\frac{1}{q_e^2} = \frac{B}{A} - \frac{1}{A}\ln C_e \tag{16}$$

where A and B are constants and can be obtained from the plot of $1/q_e^2$ and $\ln C_e$. Various isotherm models are graphicaly shown in Fig. 7. The results confirmed that adsorption of MB on MP followed Langmuir isotherm. The Langmuir isotherm showed very good fitting in terms of regression coefficient (R^2 = 0.998) and the obtained adsorption capacity is very close to experimentally determined value. Agarwal et al. [35] also found that the adsorption of MB on *Ephedra strobilacea* sawdust obeyed Langmuir adsorption isotherm.

Langmuir constant is further used to predict the dye and adsorbent interaction by using Eq. (17):

$$R_L = \left(\frac{1}{1 + K_L C_0}\right) \tag{17}$$

where R_L is a dimensionless parameter, which gives information about the adsorption of dyes on the adsorbent. There are four possible scenarios of R_L, if the adsorption is linear ($R_L = 1$), favorable ($0 < R_L < 1$), unfavorable ($R_L > 1$) or irreversible ($R_L = 0$). The calculated value of R_L using Eq. (17) is 5.7×10^{-3}; confirming that the adsorption of MB on MP is favorable.

3.6. Performance of MPs in MB removal

Table 7 shows the adsorption of MB on different biosorbents as reported by researchers [37–43]. The comparison confirms that the adsorption capacity of MB on MP is substantially higher than that of other biosorbent. Palapol et al. [36]reported high adsorption of MB using activated carbon synthesized from MP. However, the MP without any treatment has better potential to remove MB.

4. Conclusions

MPs were investigated as potential biosorbent for the removal of MB from aqueous solution. MPs showed highest adsorption capacity for MP (272.9 mg/g) at pH = 10, adsorbent dose = 0.01 g, time = 60 min and initial MB concentration 150 mg/L. Optimum number of neurons were found to be 4 for LM training algorithm with the highest value of R^2 = 0.997 and lowest MSE of 2.972. The kinetic study revealed that pseudo-second-order model was best suited

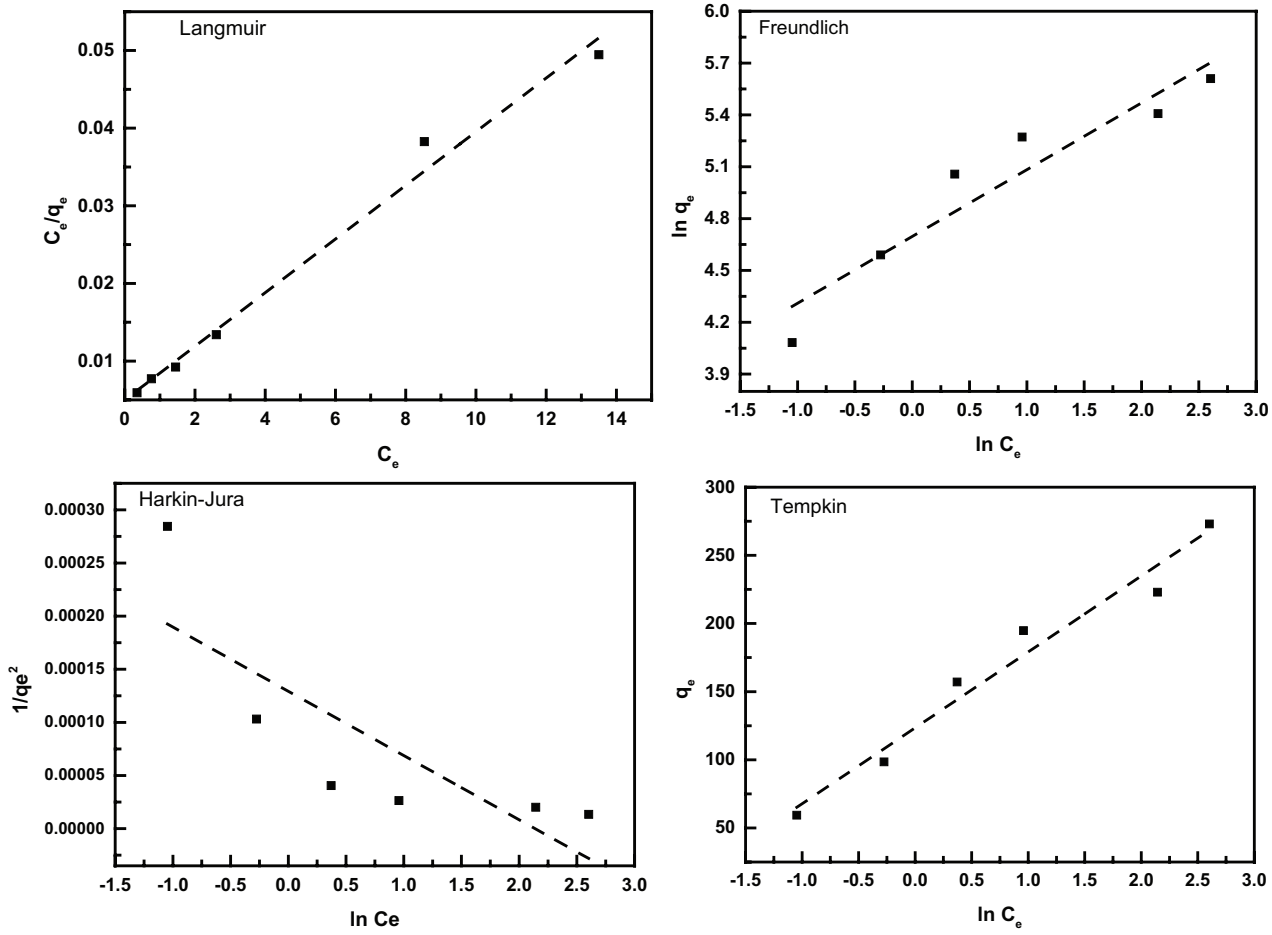

Fig. 7. Different isotherms plot for methylene blue adsorption on MP.

Table 6
Adsorption isotherm parameters calculated for MB adsorption on MPs using different adsorption isotherm models

Type	Linear form	Plot	Parameters
Langmuir	$\frac{C_e}{q_e}=\frac{1}{bQ_o}+\frac{C_e}{Q_o}$	$\frac{C_e}{q_e}\ vs\ C_e$	Q_o = 289.01 b = 1.145 R^2 = 0.998 $R_L = 5.7 \times 10^{-3}$
Freundlich	$\ln q_e=\ln K_F+\frac{1}{n}\ln C_e$	$\ln q_e\ vs\ C_e$	$1/n$ = 0.2723 K_F = 2.160 R^2 = 0.694
Temkin	$q_e = B_1 \ln k_T + B_1 \ln C_e$	$q_e\ vs\ \ln c_e$	B = 51.11 R^2 = 0.768
Harkin–Jura	$\frac{1}{q_e^2}=\frac{B}{A}-\frac{1}{A}\ln C_e$	$\frac{1}{q_e^2}\ vs\ \ln c_e$	A = –284.09 B = –2.0255 R^2 = 0.62974

(R^2 = 0.999) to describe adsorption of MB dye on MP compared with other kinetic models studied. The isotherm study showed that the adsorption phenomenon followed the Langmuir isotherm model, dominated by electrostatic interaction between adsorbent and adsorbate. The positive value of $\Delta H°$ and negative value of $\Delta G°$ confirmed that MB adsorption on the MP is spontaneous and endothermic in nature. Hence, it can be concluded that MP could be used as a potential, low cost, efficient and effective adsorbent for MB removal from aqueous solution.

Table 7
MB adsorption capacity of different biosorbents [37–43]

Biosorbent	q_t (mg/g)	Reference
Potato peel	105.26	[37]
Saw palmetto spent	71.00	[38]
Jackfruit	114.69	[39]
Broad bean peels	192.72	[40]
Pumpkin seed hull	141.92	[41]
Pineapple stem	119.05	[42]
Garlic peel (GP)	82.64	[43]
Mangosteen peel (MP)	289.01	This work

Acknowledgments

The authors gratefully acknowledge the YUTP (0153AA-A95) and Fundamental and Applied Science Department, Universiti Teknologi PETRONAS (UTP), 32610 Bander Seri Iskander, Perak, Malaysia for providing financial support for this research work.

References

[1] A. Prüss, D. Kay, L. Fewtrell, J. Bartram, Estimating the burden of disease from water, sanitation, and hygiene at a global level, Environ. Health Perspect., 110 (2002) 537–542.
[2] B. Imran, S.J. Khan, I.A. Qazi, M. Arshad, Removal and recovery of sodium hydroxide (NaOH) from industrial wastewater by two-stage diffusion dialysis (DD) and electrodialysis (ED) processes, Desal. Wat. Treat., 57 (2016) 7926–7932.
[3] V. Gupta, Application of low-cost adsorbents for dye removal–a review, J. Environ. Manage., 90 (2009) 2313–2342.
[4] N.H. Azmi, U.F.M. Ali, F. Muhammad Ridwan, K.M. Isa, N.Z. Zulkurnai, M.K. Aroua, Preparation of activated carbon using sea mango (*Cerbera odollam*) with microwave-assisted technique for the removal of methyl orange from textile wastewater, Desal. Wat. Treat., 57 (2016) 29143–29152.
[5] H. Métivier-Pignon, C. Faur-Brasquet, P. Le Cloirec, Adsorption of dyes onto activated carbon cloths: approach of adsorption mechanisms and coupling of ACC with ultrafiltration to treat coloured wastewaters, Sep. Purif. Technol., 31 (2003) 3–11.
[6] A. Nasrullah, H. Khan, A.S. Khan, Z. Man, N. Muhammad, M.I. Khan, N.M. Abd El-Salam, Potential biosorbent derived from *Calligonum polygonoides* for removal of methylene blue dye from aqueous solution, Sci. World J., 2015 (2015) 11.
[7] A. Nasrullah, H. Khan, A.S. Khan, N. Muhammad, Z. Man, F.U. Khan, Z. Ullah, *Calligonum polygonoides* biomass as a low-cost adsorbent: surface characterization and methylene blue adsorption characteristics, Desal. Wat. Treat., 57 (2016) 7345–7357.
[8] S.U. Khan, F.U. Khan, I.U. Khan, N. Muhammad, S. Badshah, A. Khan, A. Ullah, A.S. Khan, H. Bilal, A. Nasrullah, Biosorption of nickel (II) and copper (II) ions from aqueous solution using novel biomass derived from *Nannorrhops ritchiana* (Mazri Palm), Desal. Wat. Treat., 57 (2016) 3964–3974.
[9] J. Gülen, B. Akın, M. Özgür, Ultrasonic-assisted adsorption of methylene blue on sumac leaves, Desal. Wat. Treat., 57 (2016) 9286–9295.
[10] K.Y. Hor, J.M.C. Chee, M.N. Chong, B. Jin, C. Saint, P.E. Poh, R. Aryal, Evaluation of physicochemical methods in enhancing the adsorption performance of natural zeolite as low-cost adsorbent of methylene blue dye from wastewater, J. Cleaner Prod., 118 (2016) 197–209.
[11] M.I. Khan, T.K. Min, K. Azizli, S. Sufian, H. Ullah, Z. Man, Effective removal of methylene blue from water using phosphoric acid based geopolymers: synthesis, characterizations and adsorption studies, RSC Adv., 5 (2015) 61410–61420.
[12] N.S.A. Rahman, B. Azahari, M.F. Yhaya, W.R. Ismail, Crosslinking of kapok cellulose fiber via azide alkyne click chemistry as a new material for filtering system: a preliminary study, Int. J. Adv. Sci. Eng. Inform. Technol., 6 (2016) 16–19.
[13] N. Fayoud, S. Tahiri, S. Alami Younssi, A. Albizane, D. Gallart-Mateu, M. Cervera, M. de la Guardia, Kinetic, isotherm and thermodynamic studies of the adsorption of methylene blue dye onto agro-based cellulosic materials, Desal. Wat. Treat., 57 (2016) 16611–16625.
[14] H. Deng, J. Ning, X. Wang, Amino-functionalized cotton fiber for enhanced adsorption of active brilliant red X-3B from aqueous solution, Microsc. Res. Tech., 76 (2016) 1200–1207.
[15] D. Suteu, M. Badeanu, T. Malutan, A.-I. Chirculescu, Valorization of food wastes (orange seeds) as adsorbent for dye retention from aqueous medium, Desal. Wat. Treat., 57 (2016) 29070–29081.
[16] C. Saucier, M.A. Adebayo, E.C. Lima, R. Cataluña, P.S. Thue, L.D. Prola, M. Puchana-Rosero, F.M. Machado, F.A. Pavan, G. Dotto, Microwave-assisted activated carbon from cocoa shell as adsorbent for removal of sodium diclofenac and nimesulide from aqueous effluents, J. Hazard. Mater., 289 (2015) 18–27.
[17] Lagergren, S., About the theory of so-called adsorption of soluble substances, K. Sven. Vetensk. Handl., 24 (1898) 1–39.
[18] M. Alkan, Ö. Demirbaş, M. Doğan, Adsorption kinetics and thermodynamics of an anionic dye onto sepiolite, Microporous Mesoporous Mater., 101 (2007) 388–396.
[19] J. Zeldowitsch, Über den mechanismus der katalytischen oxydation von CO an MnO_2, Acta Physicochim. URSS, 1 (1934) 364–449.
[20] I. Langmuir, The constitution and fundamental properties of solids and liquids. II. Liquids, J. Am. Chem. Soc., 3 (1917) 1848–1906.
[21] H. Freundlich, Over the adsorption in solution, J. Phys. Chem., 57 (1906) e470.
[22] M. Temkin, V. Pyzhev, Kinetics of ammonia synthesis on promoted iron catalysts, Acta Physiochim. URSS, 12 (1940) 217–222.
[23] W.D. Harkins, G. Jura, Surfaces of solids. XIII. A vapor adsorption method for the determination of the area of a solid without the assumption of a molecular area, and the areas occupied by nitrogen and other molecules on the surface of a solid, J. Am. Chem. Soc., 66 (1944) 1366–1373.
[24] X. Han, W. Wang, X. Ma, Adsorption characteristics of methylene blue onto low cost biomass material lotus leaf, Chem. Eng. J., 171 (2011) 1–8.
[25] B. Hameed, A. Ahmad, Batch adsorption of methylene blue from aqueous solution by garlic peel, an agricultural waste biomass, J. Hazard. Mater., 164 (2009) 870–875.
[26] A. Gupta, C. Balomajumder, Simultaneous adsorption of Cr(VI) and phenol onto tea waste biomass from binary mixture: multicomponent adsorption, thermodynamic and kinetic study, J. Environ. Chem. Eng., 3 (2015) 785–796.
[27] N. Kannan, M.M. Sundaram, Kinetics and mechanism of removal of methylene blue by adsorption on various carbons—a comparative study, Dyes Pigm., 51 (2001) 25–40.
[28] O. Hamdaoui, E. Naffrechoux, Modeling of adsorption isotherms of phenol and chlorophenols onto granular activated carbon: part I. Two-parameter models and equations allowing determination of thermodynamic parameters, J. Hazard. Mater., 147 (2007) 381–394.
[29] M. Alkan, M. Dogan, Adsorption kinetics of Victoria blue onto perlite, Fresenius Environ. Bull., 12 (2003) 418–425.
[30] H.N. Bhatti, Q. Zaman, A. Kausar, S. Noreen, M. Iqbal, Efficient remediation of Zr(IV) using citrus peel waste biomass: kinetic, equilibrium and thermodynamic studies, Ecol. Eng., 95 (2016) 216–228.
[31] R. Kumar, M. Barakat, Decolourization of hazardous brilliant green from aqueous solution using binary oxidized cactus fruit peel, Chem. Eng. J., 226 (2013) 377–383.
[32] T. Sheela, Y.A. Nayaka, Kinetics and thermodynamics of cadmium and lead ions adsorption on NiO nanoparticles, Chem. Eng. J., 191 (2012) 123–131.

[33] F. Nekouei, H. Noorizadeh, S. Nekouei, M. Asif, I. Tyagi, S. Agarwal, V.K. Gupta, Removal of malachite green from aqueous solutions by cuprous iodide–cupric oxide nano-composite loaded on activated carbon as a new sorbent for solid phase extraction: isotherm, kinetics and thermodynamic studies, J. Mol. Liq., 213 (2016) 360–368.
[34] M. Ghaedi, A.G. Nasab, S. Khodadoust, M. Rajabi, S. Azizian, Application of activated carbon as adsorbents for efficient removal of methylene blue: kinetics and equilibrium study, J. Ind. Eng. Chem., 20 (2014) 2317–2324.
[35] S. Agarwal, I. Tyagi, V.K. Gupta, N. Ghasemi, M. Shahivand, M. Ghasemi, Kinetics, equilibrium studies and thermodynamics of methylene blue adsorption on *Ephedra strobilacea* saw dust and modified using phosphoric acid and zinc chloride, J. Mol. Liq., 218 (2016) 208–218.
[36] Y. Palapol, S. Ketsa, D. Stevenson, J.M. Cooney, A.C. Allan, I.B. Ferguson, Colour development and quality of mangosteen (*Garcinia mangostana* L.) fruit during ripening and after harvest, Postharvest Biol. Technol., 51 (2009) 349–353.
[37] E.-K. Guechi, O. Hamdaoui, Biosorption of methylene blue from aqueous solution by potato (*Solanum tuberosum*) peel: equilibrium modelling, kinetic, and thermodynamic studies, Desal. Wat. Treat., 57 (2016) 10270–10285.
[38] P.K. Papegowda, A.A. Syed, Isotherm, kinetic and thermodynamic studies on the removal of methylene blue dye from aqueous solution using saw palmetto spent, Int. J. Environ. Res., 11 (2017) 91–98.
[39] B. Hameed, Removal of cationic dye from aqueous solution using jackfruit peel as non-conventional low-cost adsorbent, J. Hazard. Mater., 162 (2009) 344–350.
[40] B. Hameed, M. El-Khaiary, Sorption kinetics and isotherm studies of a cationic dye using agricultural waste: broad bean peels, J. Hazard. Mater., 154 (2008) 639–648.
[41] B. Hameed, M. El-Khaiary, Removal of basic dye from aqueous medium using a novel agricultural waste material: pumpkin seed hull, J. Hazard. Mater., 155 (2008) 601–609.
[42] B. Hameed, R. Krishni, S. Sata, A novel agricultural waste adsorbent for the removal of cationic dye from aqueous solutions, J. Hazard. Mater., 162 (2009) 305–311.
[43] B.H. Hameed, A.A. Ahmad, Batch adsorption of methylene blue from aqueous solution by garlic peel, an agricultural waste biomass, J. Hazard. Mater., 164 (2009) 870–875.